

The Planetary Nebula Luminosity Function at the Dawn of Gaia

Robin Ciardullo¹

Abstract The [O III] $\lambda 5007$ Planetary Nebula Luminosity Function (PNLF) is an excellent extragalactic standard candle. In theory, the PNLF method should not work at all, since the luminosities of the brightest planetary nebulae (PNe) should be highly sensitive to the age of their host stellar population. Yet the method appears robust, as it consistently produces $\lesssim 10\%$ distances to galaxies of all Hubble types, from the earliest ellipticals to the latest-type spirals and irregulars. It is therefore uniquely suited for cross-checking the results of other techniques and finding small offsets between the Population I and Population II distance ladders. We review the calibration of the method and show that the zero points provided by Cepheids and the Tip of the Red Giant Branch are in excellent agreement. We then compare the results of the PNLF with those from Surface Brightness Fluctuation measurements, and show that, although both techniques agree in a relative sense, the latter method yields distances that are $\sim 15\%$ larger than those from the PNLF. We trace this discrepancy back to the calibration galaxies and argue that, due to a small systematic error associated with internal reddening, the true distance scale likely falls between the extremes of the two methods. We also demonstrate how PNLF measurements in the early-type galaxies that have hosted Type Ia supernovae can help calibrate the SN Ia maximum magnitude-rate of decline relation. Finally, we discuss how the results from space missions such as Kepler and Gaia can help our understanding of the PNLF phenomenon and improve our knowledge of the physics of local planetary nebulae.

Keywords distance scale — galaxies: distances and redshifts — planetary nebulae: general

1 Introduction

The [O III] $\lambda 5007$ Planetary Nebulae Luminosity Function (PNLF) has been a reliable and precise extragalactic distance indicator for over ~ 20 years (Jacoby 1989; Ciardullo et al. 1989a; Jacoby et al. 1992). During this time, the method has been applied to both elliptical (Jacoby et al. 1990) and spiral (Feldmeier et al. 1997) galaxies, to galactic spheroids (Ciardullo et al. 1989a; Jacoby et al. 1989; Hui et al. 1993) and disks (Feldmeier et al. 1997), and even to stars lost within the intergalactic environment of rich clusters (Feldmeier et al. 2004). In addition, PNLF observations are relatively easy: the method requires neither space-based observations nor heroically long integrations, and the photometric procedures needed to derive accurate distances are simple and straightforward. As a result, the PNLF is an integral part of the extragalactic distance ladder, and perhaps the best tool we have for examining systematic differences between Population I and Population II distance methods (see Figure 1).

Of course, no technique is perfect. The PNLF is not well-suited for small galaxies which contain few planetary nebulae, nor can it reach to ~ 100 Mpc, where the unperturbed Hubble Flow dominates. For all practical purposes, PNLF observations are limited to ~ 20 Mpc (but see Gerhard et al. (2005) and Ventimiglia et al. (2011) for PN measurements in Coma and Hydra!). The technique also requires the use of a narrow-band [O III] $\lambda 5007$ filter (FWHM ~ 50 Å), whose properties in the converging beam of a telescope are well known. In this age of fast, extremely wide-field imagers, this can be a severe limitation, especially for systems where the 5007 Å line is redshifted out of the bandpass of a rest-frame [O III] filter. Finally, the PNLF cannot easily be calibrated in the Milky Way (but see Méndez et al. (1993) and Kovacevic et al. (2011b) for attempts at a

Robin Ciardullo

The Pennsylvania State University

¹Institute for Gravitation and the Cosmos, The Pennsylvania State University

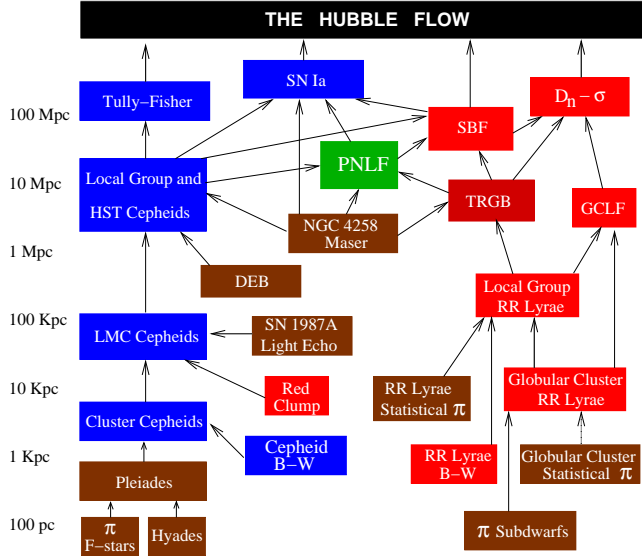


Fig. 1 The extragalactic distance ladder. The blue boxes show techniques useful in star-forming galaxies, the red boxes give methods best suited for Pop II systems, and the brown boxes represent geometric measurements. Since the PNLF is equally effective in all stellar populations, it is ideal for cross-checking the results of different methods.

local calibration), and we are far away from having a theoretical understanding of the method.

2 Why the PNLF Can't Work

The universe constantly surprises us. For example, in the 1980's, if one were to ask whether 4-m telescopes could detect [O III] $\lambda 5007$ emission from planetary nebulae in the Virgo Cluster core, the answer would have certainly been no. The main-sequence turnoff of an elliptical galaxy is $\sim 1M_{\odot}$, which, through the initial mass-final mass relation, means that the central stars of the PNe currently being produced have relatively small masses, i.e., $\sim 0.52M_{\odot}$ (Kalirai et al. 2008). It is well established that cores in this mass range cannot be more luminous than $\sim 1000 L_{\odot}$ (Schönberner 1983; Vassiliadis & Wood 1994), and that less than $\sim 12\%$ of this flux can be reprocessed into the [O III] $\lambda 5007$ emission line (Dopita et al. 1992; Schönberner et al. 2010). Thus, at maximum, the PNe inside the elliptical galaxies of Virgo should have [O III] monochromatic fluxes of 1.2×10^{-17} ergs cm^{-2} s^{-1} ($m_{5007} \sim 28.5$), well below the threshold for night-long observations with a 4-m class telescope.

Of course, one might argue that real galaxies contain a mix of stellar populations and that there will always be some PNe produced by higher mass stars. But this

claim poses another problem. As elegantly pointed out by Renzini & Buzzoni (1986), the number of PNe produced by any single-aged stellar population is linearly proportional to the luminosity of that population, i.e.,

$$N(PN) = B \cdot t \cdot L \quad (1)$$

where $t \sim 500$ yr is the lifetime of a PN in its [O III]-bright phase (Marigo et al. 2004; Schönberner et al. 2007), L is the total integrated (bolometric) luminosity of the population in question, and B is the population's luminosity specific stellar evolutionary flux. Remarkably, B does not depend on age, metallicity, or initial mass function: to within $\sim 10\%$, all populations older than ~ 1 Gyr have $B \sim 2 \times 10^{-11}$ stars $\text{yr}^{-1} L_{\odot}^{-1}$ (Renzini & Buzzoni 1986). Consequently, in order for a Virgo elliptical to have a sizeable number of [O III]-bright PNe, $\sim 10\%$ of its stars must be no older than ~ 1 Gyr. Such a result has long been ruled out via integrated light spectroscopy (e.g., Vazdekis et al. 1997; Trager et al. 2000).

Furthermore, even if the PNe were detected, there is absolutely no reason to expect the bright end of the PNLF to be a standard candle. From stellar evolution theory, the [O III] $\lambda 5007$ magnitude of the brightest PNe produced by a simple (single age) stellar population should change with time, following

$$\begin{aligned} \frac{dM_{5007}}{dt} &= \left(\frac{dM_{5007}}{d \log L_{5007}} \right) \cdot \left(\frac{d \log L_{5007}}{d \log L_*} \right) \cdot \\ &\quad \left(\frac{d \log L_*}{dm_f} \right) \cdot \left(\frac{dm_f}{dm_t} \right) \cdot \left(\frac{dm_t}{dt} \right) \\ &= (-2.5) \cdot (\sim 1) \cdot (\sim 7) \cdot (0.11) \cdot (0.8 t^{-1.4}) \\ &= \sim -1.5 t^{-1.4} \end{aligned} \quad (2)$$

where L_* is the luminosity of the central star, m_f is the mass of the PN core, m_t is the turnoff mass of the stellar population, and t is the age of the population (measured in Gyr). All these derivatives are reasonably well known via our knowledge of main sequence and post-AGB stellar evolution (e.g., Iben & Laughlin 1989; Vassiliadis & Wood 1994), the initial mass-final mass relation (e.g., Kalirai et al. 2008; Dobbie et al. 2009), and nebular physics (e.g., Ferland et al. 1998; Perinotto et al. 2004). (The most uncertain term involves the reprocessing of stellar luminosity into line emission at 5007 \AA , but models such as those by Schönberner et al. (2010) suggest that this derivative is a slowly varying quantity.) For old stellar systems ($t \sim 10$ Gyr), equation (2) implies that the PNLF cutoff should fade by ~ 0.1 mag per Gyr, and over a timescale of ~ 10 Gyr, the decline in brightness should be more than ~ 4 mag (Marigo et al. 2004; Schönberner et al.

2007). In this age of precision cosmology, such a strong dependence would have been certainly been seen.

Finally, an examination of planetary nebula morphologies in the Milky Way reveals that most bright PNe are asymmetric, and have position-dependent dust opacities within their circumstellar envelopes (e.g., Ueta et al. 2000; Siódmiak et al. 2008). The effect this dust has on the emergent [O III] $\lambda 5007$ emission is significant: although each PN is different, the average [O III]-bright planetary nebula is self-extincted by more than 0.6 mag at 5007 Å (Herrmann & Ciardullo 2009; Reid & Parker 2010). In fact, as Figure 2 shows, the bright-end cutoff of the PNLF is largely defined by the effects of sight-line dependent circumstellar extinction. At face value, this fact alone would seem to preclude the PNLF from being an effective distance indicator.

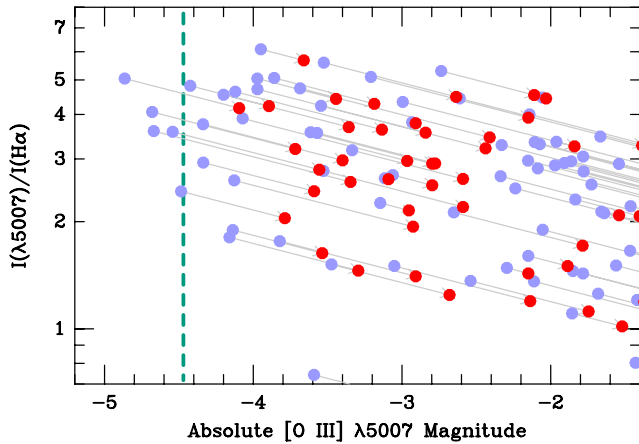


Fig. 2 The [O III] $\lambda 5007$ to $H\alpha + [N II]$ line ratio plotted against [O III] absolute magnitude for a complete sample of PNe in the LMC (Reid & Parker 2010). The light blue points show the intrinsic line strengths; the red points illustrate the line intensities that are observed. The dotted green line displays the observed value of the PNLF cutoff, M^* . The plot suggests that M^* is largely defined by the action of circumstellar dust.

3 But the PNLF Does Work

Despite these arguments, the PNLF is a precise extragalactic standard candle, capable of generating distances to better than $\sim 10\%$ in clusters as far away as Virgo and Fornax. To demonstrate this, one need only look at our Local Group neighbor, M31. As illustrated in Figure 3, the PNLF of M31’s bulge ($R < 1$ kpc) has the same bright-end cutoff (defined via the absolute magnitude M^*) as that of the system’s inner disk ($6 < R < 10$ kpc) and outer disk/halo ($R > 15$ kpc). Given the range of stellar population being observed, this invariance is remarkable.

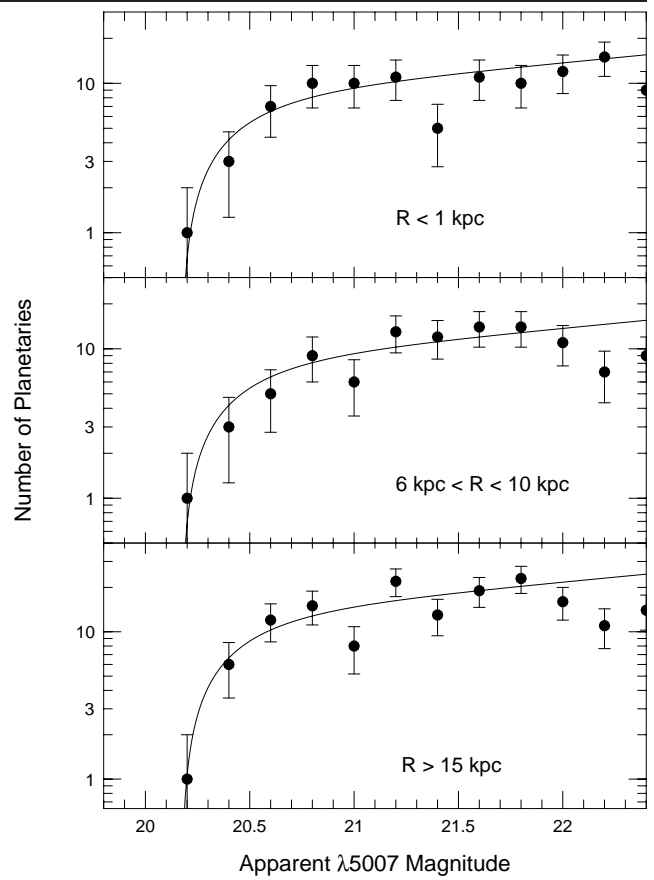


Fig. 3 The observed planetary nebula luminosity functions for samples of M31 PNe projected at three different galactocentric radii. The curves show the best-fitting empirical law. Although the stellar populations of M31’s inner bulge ($R < 1$ kpc), inner disk ($6 \text{ kpc} < R < 10$ kpc), and outer disk/halo ($R > 15$ kpc) are vastly different, the derived PNLF distances to each region are consistent to within ~ 0.05 mag.

M31 is not the only place where the PNLF has been tested. PN studies in galaxies as diverse as M33 (Ciardullo et al. 2004), NGC 5128 (Hui et al. 1993), and NGC 4494 (Jacoby et al. 1996), have been unable to detect any change in M^* with galactocentric radius. Similarly, observations of galaxies in groups and clusters, such as Triangulum (Ciardullo et al. 1991), the M81 Group (Jacoby et al. 1989; Ciardullo et al. 2002), Leo I (Ciardullo et al. 1989b; Feldmeier et al. 1997; Ciardullo et al. 2002), Virgo (Jacoby et al. 1990; Feldmeier et al. 2007), and Fornax (McMillan et al. 1993; Teodorescu et al. 2005; Feldmeier et al. 2007) (almost) always place all the galaxies comfortably within the typical group diameter of ~ 1 Mpc. (The lone exception is in Virgo, where the PNLF clearly resolves the M84/M86 system which is known to be infalling into Virgo from behind.) The multitude of internal tests place strong constraints on the types and amplitudes of

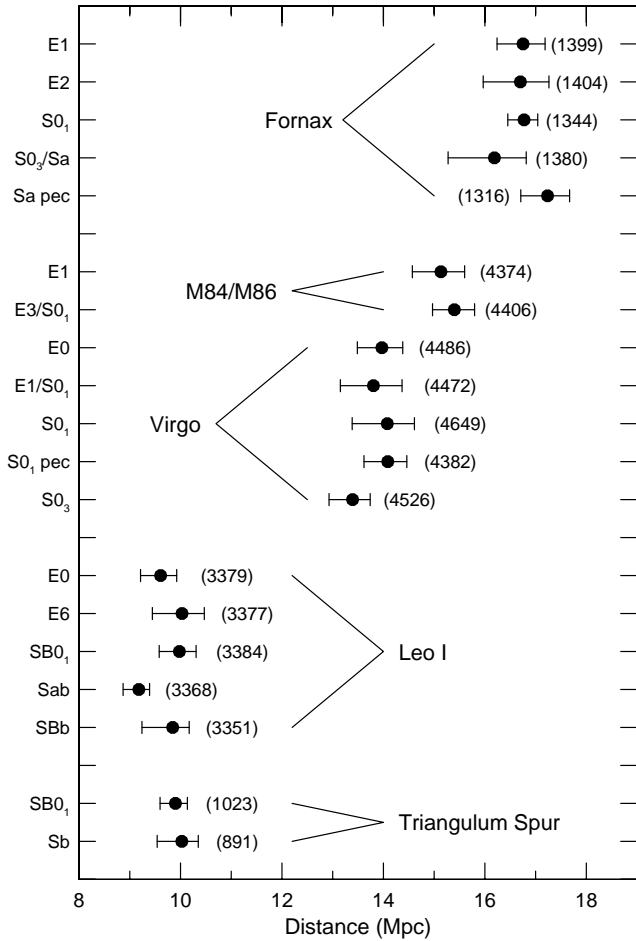


Fig. 4 PNLF distance measurements in the Triangulum Spur, the Leo I Group, the Virgo Cluster, and the Fornax Cluster. The M84/M86 system is also marked: although projected onto the Virgo Cluster core, this group is actually falling into Virgo from behind. The Hubble types are from Sandage & Tammann (1981). The diversity of Hubble types illustrates the robustness of the PNLF method.

any systematic errors that might be associated with the technique. The tests also demonstrate that the PNLF is capable of generating relative extragalactic distances to just a few percent in a variety of galactic environments.

4 The Calibration of the PNLF

There is no theoretical explanation for the constancy of the PNLF, and reliable distances to Galactic planetary nebulae are few and far between (Phillips 2004; Harris et al. 2007). Hence, the only way to obtain an absolute measurement of M^* and look for external errors in the PNLF method is to survey extragalactic systems that have distances known from other methods. Ciardullo et al. (2002) did this via PN observations inside 13 galaxies with Cepheid distances derived by the

HST Key Project (Freedman et al. 2001). By adopting the “universal” PNLF first proposed by Ciardullo et al. (1989a),

$$N(M) \propto e^{0.307M} \{1 - e^{3(M^* - M)}\} \quad (3)$$

the authors obtained a value of $M^* = -4.47$, where

$$M_{5007} = -2.5 \log F_{5007} - 13.74 \quad (4)$$

and F_{5007} is the [O III] $\lambda 5007$ flux in $\text{ergs cm}^{-2} \text{s}^{-1}$.

Remarkably, despite ~ 20 years of observations, non-parametric statistical tests such as Kolmogorov-Smirnov and Anderson-Darling still have not found any reason to reject the shape defined by this simple analytic function (but see the slitless spectroscopy of Sambhus et al. (2006) for a curious result in the elliptical galaxy NGC 4697). Of course, this does not mean that other formulations of the PNLF are not possible. For example, the recent distance determinations to NGC 4697 (Méndez et al. 2001), NGC 1344 (Teodorescu et al. 2005), M82 (Johnson et al. 2009), NGC 821 (Teodorescu et al. 2010), and NGC 4649 (Teodorescu et al. 2011) all use a numerical form of the PNLF derived by combining models of post-AGB evolution with empirical constraints on the excitation of [O III] $\lambda 5007$ in Galactic and Magellanic Cloud planetaries (Méndez & Soffner 1997). These measurements are self-consistent within themselves, and usually produce distances that are very similar to those found from equation (3). However, because the functions are different, there may be small ($\lesssim 0.1$ mag) systematic offsets between the distances derived in this way and those inferred from the purely empirical PNLF. The quoted uncertainties of the individual distances may also have slightly different meanings.

Since 2002, a few of the PNLF and Cepheid measurements have improved, and the number of galaxies studied by both methods has increased to 16. But qualitatively, little has changed. As the left-hand panel of Figure 5 illustrates, all stellar populations more metal-rich than the LMC appear to have the same value for the PNLF cutoff, $M^* \sim -4.5$. In the smaller, metal-poor systems, M^* does fade, in general agreement with the nebular model predictions of Dopita et al. (1992) and Schönberner et al. (2010). However, since these low-mass systems have few PNe and poorly defined PN luminosity functions, this systematic shift in M^* is not an important limitation of the method.

We do note that the best-fit value of M^* can be changed slightly, depending on how one models the response of the Cepheid period-luminosity relation to metallicity. The solid points displayed in the left-hand panel of Figure 5 adopt the Cepheid distances

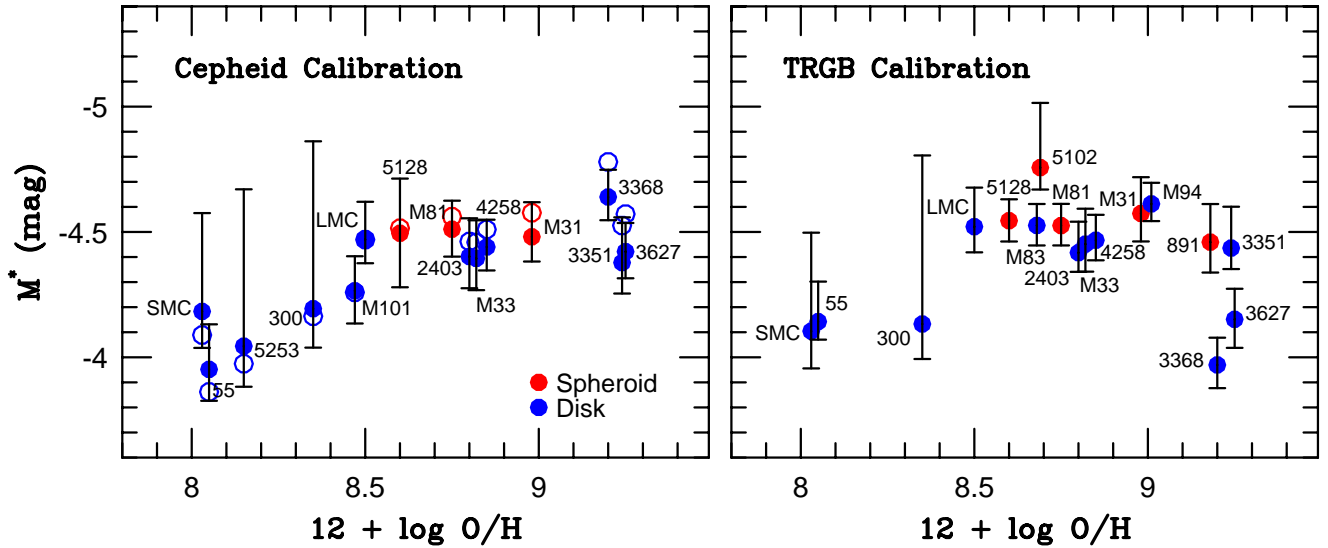


Fig. 5 Measurements of M^* derived using distance estimates from Cepheids (left panel) and the Tip of the Red Giant Branch (right panel). Most of the Cepheid distances come from Freedman et al. (2001) and assume no metallicity correction. The open circles show the same calibration with an assumed value of $\gamma = -0.2$ for the dependence of the Cepheid period-luminosity relation on metallicity. Such a correction increases M^* by ~ 0.07 mag, while increasing the dispersion only slightly. The TRGB distances come principally from Dalcanton et al. (2009), Jacobs et al. (2009), and Hislop et al. (2011).

of Freedman et al. (2001) and assume that the period-luminosity relation for Cepheids has no dependence on metallicity. If we exclude the small, low-metallicity galaxies (i.e., objects with $12 + \log O/H < 8.45$), these data imply a most likely value for the PNLF cut-off of $M^* = -4.46 \pm 0.05$ (standard deviation of the mean), and an external scatter ($\sigma = 0.16$ mag) that is fully consistent with the internal errors of the measurements. Alternatively, if the Freedman et al. (2001) period-luminosity data are used with their suggested metallicity dependence ($\gamma = -0.2$), then the most likely value of M^* brightens to $M^* = -4.53 \pm 0.04$, while the external scatter of the individual M^* measurements increases only marginally to 0.18 mag. Finally, an extreme value of $M^* = -4.68 \pm 0.09$ can be obtained if the Cepheid distances and metallicities of Saha et al. (2006) are used in the analysis. Under this assumption, however, the internal errors of the individual PNLF measurements are no longer consistent with the observed galaxy-to-galaxy scatter, which explodes to almost 0.3 mag.

Rather than relying solely on the Cepheid period-luminosity relation, we can take another route to the PNLF zero point by using distances inferred from measurements of the Tip of the Red Giant Branch (TRGB). Thanks mostly to *HST*, 18 PNLF galaxies of varying Hubble types now have reliable distances from this technique (Dalcanton et al. 2009; Jacobs et al. 2009; Hislop et al. 2011). The values of M^* based on these

measurements are shown in the right-hand panel of Figure 5. If we exclude the results from the two distant systems (NGC 3368 and 3627) where the TRGB and Cepheid distances are in conflict, the plot looks remarkably similar to that obtained from the Cepheids. As before, there is evidence for a decrease in M^* in low-luminosity, low-metallicity systems. However, in systems more metal-rich than the LMC, M^* again has a best-fit value of $M^* = -4.53 \pm 0.06$ and there is no evidence for a metallicity dependence. The fact that this number, with its small dispersion, agrees with the calibration derived from Cepheids supports the argument that the zero point of the PNLF system is secure at the $\sim 5\%$ level.

5 The PNLF and Surface Brightness Fluctuations

Both the Cepheid and TRGB methods establish the zero point of the PNLF distance scale to $\sim 5\%$. We can now use this fact to investigate the calibration of other methods, and search for systematic errors in the distance ladder. For example, the Surface Brightness Fluctuation (SBF) method is a popular way of obtaining high-precision distances to galaxies with smooth luminosity profiles, i.e., elliptical and lenticular systems (Tonry & Schneider 1988; Tonry et al. 2001). The technique is efficient, well calibrated (Tonry et al. 2001; Mei et al. 2005; Blakeslee et al. 2010), and has

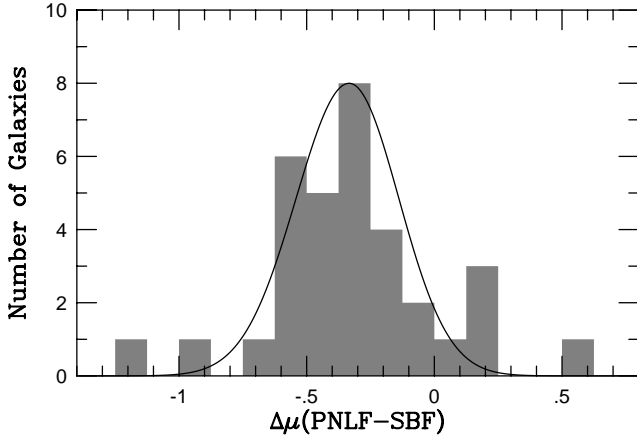


Fig. 6 A histogram of the differences between the PNLF and SBF distance moduli for 33 galaxies measured by both techniques. The two worst outliers are the edge-on galaxies NGC 4565 ($\Delta\mu = -1.14$) and NGC 891 ($\Delta\mu = +0.56$). NGC 4278 is also an outlier ($\Delta\mu = -0.97$). The curve represents the expected dispersion of the data. The figure demonstrates that, although the internal and external errors of the methods agree, the absolute scales defined by the two techniques are in conflict.

a solid theoretical foundation (e.g., Liu et al. 2000; Blakeslee et al. 2001; Marín-Franch & Aparicio 2006). The most direct way of obtaining the zero point of this method is to use the seven Cepheid galaxies with bulge populations large enough to be measured with the SBF technique. If the zero point derived from these galaxies is accurate, then a comparison of PNLF and SBF distances should show good agreement, with a mean near zero, and a scatter that is representative of the internal errors of the methods.

Figure 6 displays the difference in distance moduli for the set of 33 PNLF galaxies with SBF *I*-band measurements (Tonry et al. 2001; Blakeslee et al. 2010). It is immediately obvious that the systematic offset between the two methods is not zero, nor is it close to zero. The SBF distance scale is, in the median, $\Delta\mu = 0.33$ larger than PNLF distance scale. Moreover, this property is not restricted to the groundbased *I*-band dataset. Twelve PNLF galaxies have high-quality SBF measurements in the *z*-band from observations with the *ACS* on *HST* (Blakeslee et al. 2009); the offset between their PNLF and SBF distance moduli is $\Delta\mu = 0.42$. Similarly, 16 galaxies have PNLF and SBF *H*-band data from *HST*'s NICMOS camera (Jensen et al. 2003). The median offset between these two datasets is $\Delta\mu = 0.29$. Clearly, there is a problem with the zero point of one (or both) of the techniques.

The fact that the offset is due to a zero point error, rather than a systematic trend with stellar population or distance can be shown in two ways. First,

the solid curve in Figure 6 is not a fit to the data: it is instead, the *expected* scatter in the measurements, as determined by propagating the uncertainties associated with the individual PNLF and SBF distances and Galactic reddening. The agreement between the curve and data proves that the quoted uncertainties of both methods are reasonable, and that there is little room for additional random errors associated with the measurements. Similarly, if we plot the individual differences in distance moduli against against external parameters such as galactic absolute magnitude, color, distance modulus, or number of bright PNe (within 0.5 mag of M^*), we find only one significant trend. As Figure 7 illustrates, the offset between the PNLF and SBF correlates slightly with SBF distance modulus, in the sense that distant galaxies have smaller PNLF distances than expected from their fluctuation magnitude. Ferrarese et al. (2000) interpreted this trend as being due to a systematic error in the PNLF that only affects galaxies with distances greater than 10 Mpc. At the time, such an error could plausibly have been due to the existence of foreground intracluster stars in the clusters of Virgo and Fornax. However, in the past few years, this explanation has become untenable. Not only is the hypothesis at odds with the information provided by deep Virgo Cluster surface photometry (Mihos et al. 2005, 2009), but additional data has shown that the distance discrepancy is not restricted to galaxies in the centers of clusters. Objects such as the isolated elliptical NGC 821 and the x-ray faint elliptical NGC 4697 (in the Virgo southern extension), display the same curious offset.

In fact, a closer look at Figure 7 shows that the apparent correlation with SBF distance modulus is not driven so much by the measurements of the most distant systems, as it is by the behavior of the relatively nearby spiral galaxies. If these later-type objects are excluded from the analysis, the correlation with distance disappears. Moreover, except for the systematic offset between the two techniques, the only consistent pattern visible in Figure 7 involves the dispersion: the scatter between the PNLF and SBF distance estimates for spiral galaxies is much larger than what is seen for elliptical and lenticular systems.

So where does the offset come from? As Figure 5 demonstrates, the PNLF zero point is well calibrated by both Cepheid and TRGB measurements; while a small increase in the distance scale may be possible, any increment greater than ~ 0.1 mag is excluded by the data. Likewise, an examination of the SBF zero point calibration shows little room for error (e.g., Ajhar et al. 2001; Ferrarese et al. 2000). The median offset for the seven galaxies with both SBF and Cepheid distance determinations is $\Delta\mu = -0.10$ if the period-luminosity

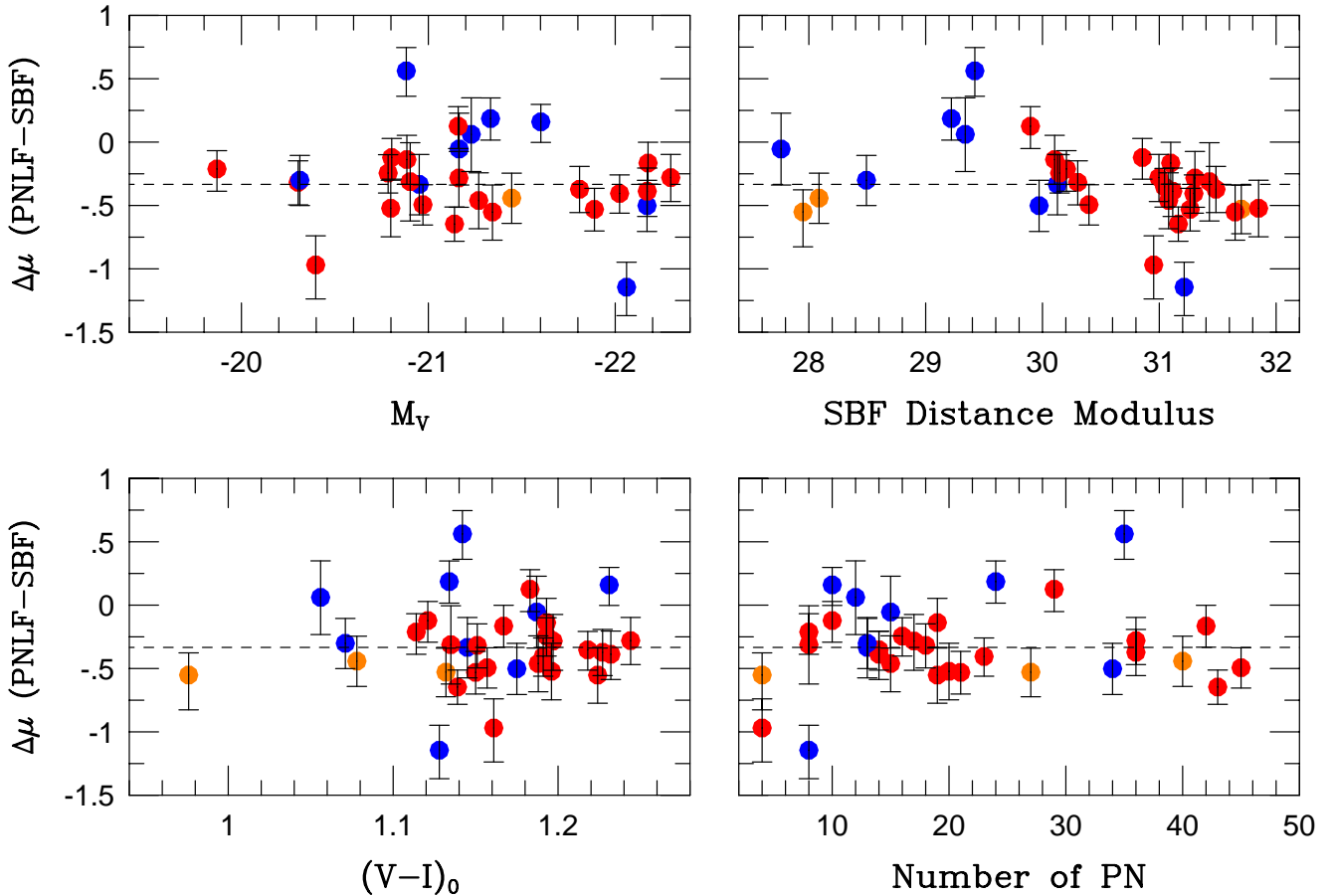


Fig. 7 The difference between SBF and PNLF distance moduli plotted against galactic absolute magnitude, distance, color, and number of PNe within 0.5 mag of M^* . The red points represent elliptical and lenticular galaxies, the orange points are gas-rich lenticulars and/or recent mergers, and the blue points are normal spiral galaxies with SBF measurements in their bulge. The correlation with SBF distance modulus, though significant ($P \sim 0.01$), disappears if spiral galaxies are excluded from the analysis. Note that the scatter for spiral galaxies is much larger than that for the early-type systems.

relation is independent of metal abundance, or $+0.08$ if $\gamma = -0.2$. It should be noted, however, that the uncertainties associated with several of the individual fluctuation magnitudes used in this calibration are large, and a similar analysis with the 12 SBF galaxies with TRGB measurements yields an offset of $\Delta\mu = -0.17$. Thus, while there is some evidence to support a modification in the SBF zero point, any downward adjustment to its distance scale must be slight, $\lesssim 0.15$ mag. Another explanation is therefore needed to reconcile the PNLF-SBF discrepancy.

The answer to this paradox is internal extinction. To calibrate an extragalactic standard candle, one needs to measure the apparent brightness of the candle, m , and adopt values for the distance modulus to the galaxy, μ , and the intervening extinction, $E(B - V)$. In other words,

$$M = m - \mu - R_\lambda E(B - V) \quad (5)$$

Here, M is the derived absolute magnitude of the standard candle in question and R_λ is the ratio of total to differential extinction at the wavelength of interest. (For [O III] $\lambda 5007$ observations of planetary nebulae, the extinction law of Cardelli et al. (1989) gives $R_\lambda = 3.5$.) For most methods, including the PNLF, if the reddening to a galaxy is underestimated, then the brightness of the standard candle will be underestimated, and the distance scale implied by the observations will be underestimated. However, in the case of the SBF technique, there is a non-negligible color term, which causes redder stellar populations to have dimmer fluctuation magnitudes. Consequently, the absolute fluctuation magnitude, \overline{M}_I , is given by

$$\overline{M}_I = C + a(V - I)_0 \quad (6)$$

where a is the slope of the color dependence. The zero-point of the SBF distance scale, represented by the con-

stant C , is therefore defined through

$$C = \overline{m}_I - \mu - a(V - I)_{\text{obs}} + (a R_V - (a+1) R_I) E(B - V) \quad (7)$$

For the I -band SBF measurements, $a = 4.5$, $R_V = 3.04$, and $R_I = 1.88$, so

$$C = \overline{m}_I - \mu + 3.34E(B - V) \quad (8)$$

(For the *HST* z -band photometry, the coefficient for the reddening term is +1.71, while for the IR fluctuation data, the value is +5.35.) So, while the response of SBF measurements to reddening has roughly the same amplitude as that of the PNLF, it has the opposite sign! Even if both analyses were performed perfectly, our imperfect knowledge of foreground extinction would cause the two distance methods to produce different results.

Of course, simple random uncertainties in the estimates of foreground reddening, such as those associated with the extinction maps of Schlegel et al. (1998), should not produce a systematic error between the two distance scales. However, the calibrators for the SBF and PNLF techniques are mostly mid-type spiral galaxies, while the vast majority of the methods' program objects are elliptical and lenticular systems. This population difference *can* create a systematic bias between the two systems. If the calibrator galaxies have, on average, as little as $E(B - V) \sim 0.02$ more internal reddening than the early-type systems that are the methods' main targets, the result will be a 0.15 mag offset between the PNLF and SBF distances, in exactly the direction that is observed. This seems quite plausible, especially since the bulges of most mid-type spirals exhibit more evidence for dust than do the interiors of normal elliptical galaxies (Windhorst et al. 2002). In fact, given the extremely strong amplitude of the extinction dependence, it would be surprising if there weren't an offset!

From the above arguments, it seems clear that the offset between the PNLF and SBF distance scales is likely the result of several small effects: a slight ($\lesssim 0.1$ mag) underestimate in the brightness of the PNLF cutoff, a slight ($\lesssim 0.2$ mag) overestimate in the zero point of the SBF method, and a small shift in both the PNLF and SBF caused by the systematically larger dust content of spiral bulges. Without the cross-checking ability of the PNLF, such subtle effects could easily go unnoticed.

6 The PNLF and SN Ia

Over 50 galaxies currently have robust PNLF distance measurements. These galaxies have hosted ~ 50 known

supernovae in the past century, and about half of these objects have well-observed light curves. Included in this sample of well-studied supernovae are 6 SN II-P, 2 SN II-L, 1 SN IIb, 1 SN IIn, 1 SN Ib, 1 SN Ic, and 13 SN Ia (see Table 1). The latter can be used to derive an estimate of H_0 .

Table 1 SN Ia in PNLF Galaxies

SN Ia	Host	Comment
1972E	NGC 5253	Photoelectric Photometry
1980N	NGC 1316	Photoelectric Photometry
1981D	NGC 1316	Photoelectric Photometry
1986G	NGC 5128	High Internal Extinction
1989B	NGC 3627	
1991bg	NGC 4374	Subluminous
1992A	NGC 1380	
1994D	NGC 4526	
1998bu	NGC 3368	
2006dd	NGC 1316	
2006mr	NGC 1316	Subluminous
2007on	NGC 1404	
2011fe	NGC 5457	

Figure 8 displays the V -band maximum magnitude-rate of decline relation for a set of well-observed supernovae in the Hubble flow, i.e., in the redshift range $0.01 < z < 0.08$ (Hicken et al. 2009), under the assumption that $H_0 = 70$ km s $^{-1}$ Mpc $^{-1}$. Also plotted are the maximum absolute magnitudes of 13 well-observed local SN Ia, using distances derived from the PNLF. The agreement between the two sets of data is surprising good, especially when one considers that several of the supernovae are from the era prior to CCD measurements and another is affected by high internal extinction. This consistency demonstrates the viability of the PNLF as a SN Ia calibrator, and its utility. Over half the local supernovae plotted in the figure occurred in early-type galaxies with no significant Population I component. Cepheids cannot be used to measure the distances to these objects. In order to study the brightnesses of SN Ia across galaxy types, one needs a method such as the PNLF, as it is the most direct way to link measurements within Population I and Population II stellar systems.

7 Prospects for the Future

The greatest impediment to improving the PNLF distance scale is the lack of an adequate theory to explain why the technique is so robust. The constancy of the PNLF cutoff cannot be explained by single-star stellar

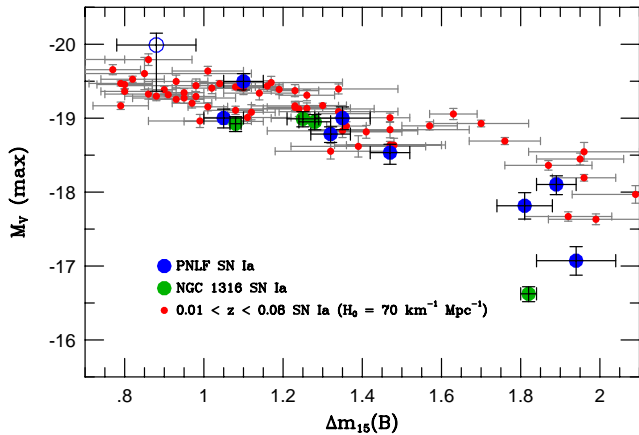


Fig. 8 The absolute V magnitudes of 13 SN Ia located within galaxies with PNLF distances, plotted against the amount of fading which occurred in the first 15 days after maximum. For comparison, a sample of supernovae in the redshift range $0.01 < z < 0.08$ is also shown, under the assumption of $H_0 = 70 \text{ km s}^{-1} \text{ Mpc}^{-1}$. Except for SN 1972E (in NGC 5253, shown as an open circle), all the supernovae are from the past 30 years.

evolution: the energy emitted by an M^* planetary nebula demands that the PN has a core mass of at least $\sim 0.6M_\odot$ (Vassiliadis & Wood 1994), and old stellar populations simply cannot produce such high-mass objects. The progenitors of $\sim 0.6M_\odot$ white dwarfs are main-sequence stars with masses $M \sim 2M_\odot$ (Kalirai et al. 2008), and stars such as these have very short main sequence lifetimes ($\tau \lesssim 1 \text{ Gyr}$; Iben & Laughlin 1989). While early-type galaxies may contain a small number of intermediate-age stars (Kaviraj et al. 2007), this population is not nearly large enough to produce the number of PNe actually observed. Consequently, in order to explain the PNLF of elliptical galaxies, a more exotic channel of stellar evolution must be considered.

Binary evolution is the likely solution to this problem. There is now considerable evidence to suggest that a significant fraction of PNe form via binary star interactions (Soker 2006; Moe & De Marco 2006). Indeed, Ciardullo et al. (2005) has proposed that an important channel for the creation of an [O III]-bright PN involves conservative mass transfer whilst on the main sequence (McCrea 1964), and the subsequent creation of a blue straggler star. Though this hypothesis is difficult to test, clues as to its viability may soon be provided by astrometric and photometric space missions. Clarkson et al. (2011) have shown that space-based astrometry of the Galactic bulge can provide a census of blue stragglers in a collisionless stellar environment with a well-studied PN population (Pottasch 1990; Kovacevic et al. 2011a). By comparing the PN

and blue straggler number densities to their expected lifetimes (e.g., Schönberner et al. 2010; Lombardi et al. 2002), one can test whether the stellar merger hypothesis is self-consistent. Similarly, if blue straggler evolution is an important channel for populating the bright end of the planetary nebula luminosity function, it must also be a significant contributor to the A-star population of the solar neighborhood. Asteroseismological studies, such as those being performed with the Kepler satellite (Balona et al. 2011), may be able to disentangle the two evolutionary scenarios, thereby shedding light on the creation rate of coalesced objects.

Another advance that we can look forward to is an improved distance scale to PNe in the Milky Way. Most Galactic planetary nebulae have distance estimates based on such dubious methods as the amount of foreground extinction (Giammanco et al. 2011) or the statistical correlation between nebular emission and nebular size (e.g., Shklovsky 1956; van de Steene & Zijlstra 1995). Factor of ~ 2 errors in these estimates are not uncommon, even for bright, well-observed objects, and as a result, obtaining a local calibration of the PNLF cutoff is extremely difficult (Méndez et al. 1993; Kovacevic et al. 2011b). This will soon change, however, as Gaia will expand the number of PNe with reliable parallax measurements from ~ 20 (Harris et al. 2007) to more than ~ 200 . This should facilitate dozens of studies of the local PN population, including its [O III] luminosity function.

Unfortunately, a Gaia-based luminosity function, by itself, will probably not enable us to significantly improve the calibration of the PNLF. As Figure 2 illustrates, M^* is highly dependent on the amount of extinction produced by circumstellar dust, and, despite the extraordinary progress made in understanding the physics of the planetary nebula phenomenon (Schönberner et al. 2010), this component of the problem has yet to be modeled. This is major issue, since observations of Galactic PNe are affected not only by the actions of circumstellar dust, but by foreground extinction as well. The problem of disentangling the two reddening components may ultimately limit any attempt to calibrate the planetary nebula luminosity function in the Milky Way.

8 Conclusion

The PNLF is neither a primary distance indicator nor a method that can reach out of the Local Supercluster into the Hubble Flow. It has no theoretical basis, and next generation missions such as Gaia will not substantially improve its calibration. Yet the technique remains an important part of the extragalactic distance

ladder: it is, perhaps, the best tool we have for linking the Population I and Population II distance scales, and identifying systematic offsets between the different methods. Moreover, it is still a relatively efficient technique that does not require space-based observations or extremely long exposure times. Since PNLF distances are often produced as a by-product of kinematic studies (i.e., Herrmann et al. 2008; Teodorescu et al. 2010), the method is likely to be producing distance measurements for years to come.

Acknowledgements We would like to thank the meeting's organizers for supporting this review. This work was supported by NSF grant AST 06-07416.

References

- Ajhar, E.A., Tonry, J.L., Blakeslee, J.P., Riess, A.G., & Schmidt, B.P. 2001, *Astrophys. J.*, 559, 584
- Balona, L.A., Cunha, M.S., Kurtz, D.W., Brandão, I.M., Gruberbauer, M., Saio, H., Östensen, R., Elkin, V.G., Borucki, W.J., Christensen-Dalsgaard, J., Kjeldsen, H., Koch, D.G., & Bryson, S.T. 2011, *Mon. Not. R. Astron. Soc.*, 410, 517
- Blakeslee, J.P., Vazdekis, A., & Ajhar, E.A. 2001, *Mon. Not. R. Astron. Soc.*, 320, 193
- Blakeslee, J.P., Cantiello, M., Mei, S., Côté, P., Barber De Graaff, R., Ferrarese, L., Jordán, A., Peng, E.W., Tonry, J.L., & Worthey, G. 2010, *Astrophys. J.*, 724, 657
- Blakeslee, J.P., Jordán, A., Mei, S., Côté, P., Ferrarese, L., Infante, L., Peng, E.W., Tonry, J.L., & West, M.J. 2009, *Astrophys. J.*, 694, 556
- Cardelli, J.A., Clayton, G.C., & Mathis, J.S. 1989, *Astrophys. J.*, 345, 245
- Ciardullo, R., Jacoby, G.H., Ford, H.C., & Neill, J.D. 1989a, *Astrophys. J.*, 339, 53
- Ciardullo, R., Jacoby, G.H., & Ford, H.C. 1989b, *Astrophys. J.*, 344, 715
- Ciardullo, R., Jacoby, G.H., & Harris, W.E. 1991, *Astrophys. J.*, 383, 487
- Ciardullo, R., Feldmeier, J.J., Jacoby, G.H., Kuzio de Naray, R., Laychak, M.B., & Durrell, P.R. 2002, *Astrophys. J.*, 577, 31
- Ciardullo, R., Sigurdsson, S., Feldmeier, J.J., & Jacoby, G.H. 2005, *ApJ*, 629, 499
- Ciardullo, R., Durrell, P.R., Laychak, M.B., Herrmann, K.A., Moody, K., Jacoby, G.H., & Feldmeier, J.J. 2004, *Astrophys. J.*, 614, 167
- Clarkson, W.I., Sahu, K.C., Anderson, J., Rich, R.M., Smith, T.E., Brown, T.M., Bond, H.E., Livio, M., Minniti, D., Renzini, A., & Zoccali, M. 2011, *Astrophys. J.*, 735, 37
- Dalcanton, J.J., Williams, B.F., Seth, A.C., Dolphin, A., Holtzman, J., Rosema, K., Skillman, E.D., Cole, A., Girardi, L., Gogarten, S.M., Karachentsev, I.D., Olsen, K., Weisz, D., Christensen, C., Freeman, K., Gilbert, K., Gallart, C., Harris, J., Hodge, P., de Jong, R.S., Karachentseva, V., Mateo, M., Stetson, P.B., Tavarez, M., Zaritsky, D., Governato, F., & Quinn, T. 2009, *Astrophys. J. Suppl. Ser.*, 183, 67
- Dobbie, P.D., Napiwotzki, R., Burleigh, M.R., Williams, K.A., Sharp, R., Barstow, M.A., Casewell, S.L., & Hubeny, I. 2009, *Mon. Not. R. Astron. Soc.*, 395, 2248
- Dopita, M.A., Jacoby, G.H., & Vassiliadis, E. 1992, *Astrophys. J.*, 389, 27
- Feldmeier, J.J., Ciardullo, R., & Jacoby, G.H. 1997, *Astrophys. J.*, 479, 231
- Feldmeier, J.J., Ciardullo, R., Jacoby, G.H., & Durrell, P.R. 2004, *Astrophys. J.*, 615, 196
- Feldmeier, J.J., Jacoby, G.H., & Phillips, M.M. 2007, *Astrophys. J.*, 657, 76
- Ferland, G.J., Korista, K.T., Verner, D.A., Ferguson, J.W., Kingdon, J.B., & Verner, E.M. 1998, *Publ. Astron. Soc. Pac.*, 110, 761
- Ferrarese, L., Mould, J.R., Kennicutt, R.C., Jr., Huchra, J., Ford, H.C., Freedman, W.L., Stetson, P.B., Madore, B.F., Sakai, S., Gibson, B.K., Graham, J.A., Hughes, S.M., Illingworth, G.D., Kelson, D.D., Macri, L., Sebo, K., & Silbermann, N.A. 2000, *Astrophys. J.*, 529, 745
- Freedman, W.L., Madore, B.F., Gibson, B.K., Ferrarese, L., Kelson, D.D., Sakai, S., Mould, J.R., Kennicutt, R.C. Jr., Ford, H.C., Graham, J.A., Huchra, J.P., Hughes, S.M.G., Illingworth, G.D., Macri, L.M., & Stetson, P.B. 2001, *Astrophys. J.*, 553, 47
- Gerhard, O., Arnaboldi, M., Freeman, K.C., Kashikawa, N., Okamura, S., & Yasuda, N. 2005, *Astrophys. J. Lett.*, 621, L93
- Giammanco, C., Sale, S.E., Corradi, R.L.M., Barlow, M.J., Viironen, K., Sabin, L., Santander-García, M., Frew, D.J., Greimel, R., Miszalski, B., Phillipps, S., Zijlstra, A.A., Mampaso, A., Drew, J.E., Parker, Q.A., & Napiwotzki, R. 2011, *Astron. Astrophys.*, 525, A58
- Harris, H.C., Dahn, C.C., Canzian, B., Guetter, H.H., Leggett, S.K., Levine, S.E., Luginbuhl, C.B., Monet, A.K.B., Monet, D.G., Pier, J.R., Stone, R.C., Tillemann, T., Vrba, F.J., & Walker, R.L. 2007, *Astron. J.*, 133, 631
- Herrmann, K.A., Ciardullo, R., Feldmeier, J.J., & Vinciguerra, M. 2008, *Astrophys. J.*, 683, 630
- Herrmann, K.A., & Ciardullo, R. 2009, *Astrophys. J.*, 703, 894
- Hicken, M., Wood-Vasey, W.M., Blondin, S., Challis, P., Jha, S., Kelly, P.L., Rest, A., & Kirshner, R.P. 2009, *Astrophys. J.*, 700, 1097
- Hislop, L., Mould, J., Schmidt, B., Bessell, M.S., Da Costa, G., Francis, P., Keller, S., Tisserand, P., Rapoport, S., Casey, A. 2011, *Astrophys. J.*, 733, 75
- Hui, X., Ford, H.C., Ciardullo, R., & Jacoby, G.H. 1993, *Astrophys. J.*, 414, 463
- Iben, I., Jr., & Laughlin, G. 1989, *Astrophys. J.*, 341, 312
- Jacobs, B.A., Rizzi, L., Tully, R.B., Shaya, E.J., Makarov, D.I., & Makarova, L. 2009, *Astron. J.*, 138, 332
- Jacoby, G.H. 1989, *Astrophys. J.*, 339, 39
- Jacoby, G.H., Ciardullo, R., Booth, J., & Ford, H.C. 1989, *Astrophys. J.*, 344, 704
- Jacoby, G.H., Ciardullo, R., & Ford, H.C. 1990, *Astrophys. J.*, 356, 332
- Jacoby, G.H., Branch, D., Ciardullo, R., Davies, R.L., Harris, W.E., Pierce, M.J., Pritchet, C.J., Tonry, J.L., & Welch, D.L. 1992, *Publ. Astron. Soc. Pac.*, 104, 599
- Jacoby, G.H., Ciardullo, R., & Harris, W.E. 1996, *Astrophys. J.*, 462, 1
- Jensen, J.B., Tonry, J.L., Barris, B.J., Thompson, R.I., Liu, M.C., Rieke, M.J., Ajhar, E.A., & Blakeslee, J.P. 2003, *Astrophys. J.*, 583, 712
- Johnson, L.C., Méndez, R.H., & Teodorescu, A.M. 2009, *Astrophys. J.*, 697, 1138
- Kalirai, J.S., Hansen, B.M.S., Kelson, D.D., Reitzel, D.B., Rich, R.M., & Richer, H.B. 2008, *Astrophys. J.*, 676, 594
- Kaviraj, S., Schawinski, K., Devriendt, J.E.G., Ferreras, I., Khochfar, S., Yoon, S.-J., Yi, S.K., Deharveng, J.-M., Boselli, A., Barlow, T., Conrow, T., Forster, K., Friedman, P.G., Martin, D.C., Morrissey, P., Neff, S., Schiminovich, D., Seibert, M., Small, T., Wyder, T., Bianchi, L., Donas, J., Heckman, T., Lee, Y.-W., Madore, B., Miliard, B., Rich, R.M., & Szalay, A. 2007, *Astrophys. J. Suppl. Ser.*, 173, 619

- Kovacevic, A.V., Parker, Q.A., Jacoby, G.H., Sharp, R., Miszalski, B., & Frew, D.J. 2011, *Mon. Not. R. Astron. Soc.*, 414, 860
- Kovacevic, A.V., Parker, Q.A., Jacoby, G.H., & Miszalski, B. 2011, *Asymmetric Planetary Nebulae 5 Conference*, arXiv:1010.1655
- Liu, M.C., Charlot, S., & Graham, J.R. 2000, *Astrophys. J.*, 543, 644
- Lombardi, J.C., Warren, J.S., Rasio, F.A., Sills, A., & Warren, A.R. 2002, *Astrophys. J.*, 568, 939
- Marigo, P., Girardi, L., Weiss, A., Groenewegen, M.A.T., & Chiosi, C. 2004, *Astron. Astrophys.*, 423, 995
- Marín-Franch, A., & Aparicio, A. 2006, *Astron. Astrophys.*, 450, 979
- McCrea, W.H. 1964, *Mon. Not. R. Astron. Soc.*, 128, 147
- McMillan, R., Ciardullo, R., & Jacoby, G.H. 1993, *Astrophys. J.*, 416, 62
- Mei, S., Blakeslee, J.P., Tonry, J.L., Jordán, A., Peng, E.W., Côté, P., Ferrarese, L., West, M.J., Merritt, D., Milosavljević, M. 2005, *Astrophys. J.*, 625, 121
- Méndez, R.H., Kudritzki, R.P., Ciardullo, R., & Jacoby, G.H. 1993, *Astron. Astrophys.*, 275, 534
- Méndez, R.H., & Soffner, T. 1997, *Astron. Astrophys.*, 321, 898
- Méndez, R.H., Riffeser, A., Kudritzki, R.-P., Matthias, M., Freeman, K.C., Arnaboldi, M., Capaccioli, M., & Gerhard, O.E. 2001, *Astrophys. J.*, 563, 135
- Mihos, J.C., Harding, P., Feldmeier, J., & Morrison, H. 2005, *Astrophys. J. Lett.*, 631, L41
- Mihos, J.C., Janowiecki, S., Feldmeier, J.J., Harding, P., & Morrison, H. 2009, *Astrophys. J.*, 698, 1879
- Moe, M., & De Marco, O. 2006, *Astrophys. J.*, 650, 916
- Perinotto, M., Schönberner, D., Steffen, M., & Calonaci, C. 2004, *Astron. Astrophys.*, 414, 993
- Phillips, J.P. 2004, *Mon. Not. R. Astron. Soc.*, 353, 589
- Pottasch, S.R. 1990, *Astron. Astrophys.*, 236, 231
- Reid, W.A., & Parker, Q.A. 2010, *Mon. Not. R. Astron. Soc.*, 405, 1349
- Renzini, A. & Buzzoni, A. 1986, *Spectral Evolution of Galaxies (Astrophysics and Space Science Library)*, Vol. 122, ed. C. Chiosi & A. Renzini (Dordrecht: Reidel), 195
- Saha, A., Thim, F., Tammann, G.A., Reindl, B., & Sandage, A. 2006, *Astrophys. J. Suppl. Ser.*, 165, 108
- Sambhus, N., Gerhard, O., & Méndez, R.H. 2006, *Astron. J.*, 131, 837
- Sandage, A., & Tammann, G.A. 1981, *A Revised Shapley-Ames Catalog of Bright Galaxies*, Washington, D.C., Carnegie Inst. of Washington
- Schoenberner, D. 1983, *Astrophys. J.*, 272, 708
- Schönberner, D., Jacob, R., Steffen, M., & Sandin, C. 2007, *Astron. Astrophys.*, 473, 467
- Schönberner, D., Jacob, R., Sandin, C., & Steffen, M. 2010, *Astron. Astrophys.*, 523, A86
- Schlegel, D.J., Finkbeiner, D.P., & Davis, M. 1998, *Astrophys. J.*, 500, 525
- Shklovsky, I.S. 1956, *Astron. Zh.* 33, 222
- Siódmiak, N., Meixner, M., Ueta, T., Sugerman, B.E.K., Van de Steene, G.C., & Szczerba, R. 2008, *Astrophys. J.*, 677, 382
- Soker, N. 2006, *Astrophys. J. Lett.*, 645, L57
- Teodorescu, A.M., Méndez, R.H., Bernardi, F., Thomas, J., Das, P., & Gerhard, O. 2011, *Astrophys. J.*, 736, 65
- Teodorescu, A.M., Méndez, R.H., Saglia, R.P., Riffeser, A., Kudritzki, R.-P., Gerhard, O.E., & Kleyna, J. 2005, *Astrophys. J.*, 635, 290
- Teodorescu, A.M., Méndez, R.H., Bernardi, F., Riffeser, A., & Kudritzki, R.P. 2010, *Astrophys. J.*, 721, 369
- Tonry, J.L., Dressler, A., Blakeslee, J.P., Ajhar, E.A., Fletcher, A.B., Luppino, G.A., Metzger, M.R., & Moore, C.B. 2001, *Astrophys. J.*, 546, 681
- Tonry, J., & Schneider, D.P. 1988, *Astron. J.*, 96, 807
- Trager, S.C., Faber, S.M., Worthey, G., & González, J.J. 2000, *Astron. J.*, 119, 1645
- Ueta, T., Meixner, M., & Bobrowsky, M. 2000, *Astrophys. J.*, 528, 861
- van de Steene, G.C., & Zijlstra, A.A. 1995, *Astron. Astrophys.*, 293, 541
- Vassiliadis, E., & Wood, P.R. 1994, *Astrophys. J. Suppl. Ser.*, 92, 125
- Vazdekis, A., Peletier, R.F., Beckman, J.E., & Casuso, E. 1997, *Astrophys. J. Suppl. Ser.*, 111, 203
- Ventimiglia, G., Arnaboldi, M., & Gerhard, O. 2011, *Astron. Astrophys.*, 528, A24
- Windhorst, R.A., Taylor, V.A., Jansen, R.A., Odewahn, S.C., Chiarenza, C.A.T., Conselice, C.J., de Grijs, R., de Jong, R.S., MacKenty, J.W., Eskridge, P.B., Frogel, J.A., Gallagher, J.S., III, Hibbard, J.E., Matthews, L.D., & O'Connell, R.W. 2002, *Astrophys. J. Suppl. Ser.*, 143, 113